Contents lists available at ScienceDirect

Comptes Rendus Chimie

Full paper/Mémoire

Removal of uranium (VI) from nuclear effluents onto aluminophosphate and silicoaluminophosphate molecular sieves

Naima Bayou [a], *, Hamid Aït-Amar [b], Mouloud Attou [c], Safia Menacer [a]

[a] Department of Management and Treatment of Radioactive Waste, Nuclear Safety Division and Radioprotection, Nuclear Research Center of Draria, BP 43, Sébala 16050, Draria, Algiers, Algeria
[b] Laboratory of Science in Industrial Process Engineering, University of Sciences and Technology Houari Boumediene, USTHB, BP 32, 16111 El-Alia, Algiers, Algeria
[c] Engineering Division of Processes and Materials, Nuclear Research Center of Draria, BP 43, Sébala 16050, Draria, Algiers, Algeria

A B S T R A C T

Aluminophosphate and silicoaluminophosphate molecular sieves with both five (AFI) and eleven (AEL) type structures are synthesized by hydrothermal crystallization at 473 K, using tripropylamine and dipropylamine as a structure-directing template. The as-prepared AFI and AEL sieves are characterized and then assessed as *sorbents* for uranium (VI) from radioactive effluents. The sorption process is used to reduce the volumes of effluents and convert them into a stable solid waste. The batch experimental studies are carried out to evaluate the AEL and AFI structure effect on the removal of uranium. The AlPO$_4$-5, SAPO-5, AlPO$_4$-11 and SAPO-11 are applied to radioactive effluents with different activities obtained from Nuclear Research Center of Draria, Algeria. Important *decontamination factor* values are obtained for AFI sorbents. Thermodynamic parameters, namely, the enthalpy (ΔH), entropy (ΔS) and free energy (ΔG) for each sorption process are calculated. The collected results indicated that sorbents are effective materials for the removal of uranium (VI) ions, the sorbent with AFI structure being a highly effective material for the removal of uranium (VI) ions from nuclear effluents.

© 2017 Académie des sciences. Published by Elsevier Masson SAS. All rights reserved.

1. Introduction

Porous zeolite-like aluminophosphate (AlPO$_4$-n) molecular sieves have attracted much interest since the first synthesis by Wilson in 1982 [1] because of their catalytic and *effective* sportive properties (chemical affinity of form and size, porosity and high sorption capacity). These molecular sieves constitute a material with selective sorption properties based on molecular size and shape difference. AlPO$_4$-n contain several structures including zeolite topological analogues and a large number of novel structures [2]. Isomorphous substitution of their Si (IV) by P (V) leads

to the synthesis of new materials abbreviated as SAPO-n and create a negative charge in the framework, which considerably influences their mechanism and capacity sorption [3]. The AFI structure consists of one-dimensional 12-membered ring pores (7.3 × 7.3 Å in size) and 10-membered ring pores (6.5 × 4.0 Å) for AEL structure [4]. These channels are larger than the diameter of the hydrated uranyl (6.5 Å) allowing its sorption by AFI and AEL materials [5]. The trapping of uranium within the structural gaps of AFI and AEL materials reduced volumes of radioactive effluents and convert it to a stable solid waste [6].

Uranium is a long-lived radioelement *present* in various radioactive liquid wastes. It is hazardous because of both its chemical toxicity and radioactivity [7]. Several techniques have been used for effluent decontamination. These include

* Corresponding author.
  E-mail address: naima_bayou@yahoo.fr (N. Bayou).

chemical precipitation, membrane-based separation, solvent extraction, ion exchange and *sorption* [8,9]. Among these techniques, sorption is often preferred because of its low cost and high removal efficiency [10]. The sorption of uranium onto various solids is a current process used in the purification of environmental and radioactive waste disposal [11]. Indeed, a large number of studies have focused on the use of natural and synthetic zeolites [12–17]. Inorganic sorbents such as zeolites are considered to be backfill materials in the safe processing of nuclear wastes because of their ability in retarding the release of radionuclides in the environment [18]. The aim of the present study is to highlight the effectiveness of porous zeolite-like aluminophosphate and silicoaluminophosphate with AFI and AEL structures for radioactive waste management.

2. Experimental section

2.1. Chemicals and reagents

All of the reagents used for the experiments are of analytical grade.

The synthetic stock uranium solution of 1 g/L at pH 3.5 was prepared by dissolving the appropriate amount of uranyl nitrate hexahydrated salt, $UO_2(NO_3)_2 \cdot 6H_2O$ (99%, Merck), in distilled water with 1 mL of nitric acid. Experimental uranium solutions of concentrations 50, 100 and 150 mg/L were obtained by dilution with distilled water.

2.2. Synthesis and characterization of $AlPO_4$-5, SAPO-5, $AlPO_4$-11 and SAPO-11 sorbents

$AlPO_4$-5, SAPO-5, $AlPO_4$-11 and SAPO-11 sorbents are synthesized hydrothermally according to the literature [2,19]. The gel composition for $AlPO_4$-*n* and SAPO-*n* sorbents is Al_2O_3, 1 P_2O_5, and 1.4 R, 50 H_2O and 0.8 Al_2O_3, 1 P_2O_5, 1.4 R, 0.2 SiO_2, 50 H_2O, respectively. The direct-structuring agents (R) used for AFI and AEL structures are tripropylamine and dipropylamine (99%, Fluka), respectively. The aluminium, silicon and phosphorous sources are pseudoboehmite catapal B (69%, Vista), aerosil SiO_2 (100%, Deggusa) and phosphoric acid (85%, Merck), respectively. The gels are introduced into 120 mL Teflon lined stainless steel autoclaves and heated at 473 K under autogenic pressure for 24 and 48 h for AFI and AEL sorbents, respectively. After the heat treatment, the autoclave is cooled in water. The resulting solids are separated by filtration, washed with distilled water and dried at 353 K overnight. The synthesized materials are calcined at 823 K for 6 h to remove the organic template.

The structural analysis is performed using X-ray diffractometer, Philips X'PERT SW powder diffractometer, with Cu $K\alpha_1$ radiation ($k = 1.54060$ Å).

The nitrogen adsorption–desorption measurements are made using a Quantachrome Nova 3200e surface analyser at 77 K. The surface areas of synthesized sorbents are obtained by the Brunauer–Emmett–Teller (BET) method. The chemical compositions are investigated by X-ray fluorescence spectrometer type MAGIX Pro. The calculated charge by TO_2 of a silicoaluminophosphate material with a composition form, $[Si^{4+}]_x[Al^{3+}]_y[P^{5+}]_zO_2$, is equal to $4x + 3y + 5z + (-2) \times 2$, where *x*, *y*, *z*, 2 are the molar fractions of Si,

Al, P and O and 4, 3, 5 and −2 are the charge of Si, Al, P and O, respectively.

The elements' composition of the effluents is investigated by a GBC Avanta Sigma-type atomic absorption spectrophotometer.

2.3. Sorption experiments

The sorption of uranium (VI) onto synthesized $AlPO_4$-5, SAPO-5, $AlPO_4$-11 and SAPO-11 is studied using the batch technique. The batch sorption is performed by agitating in a thermostat water bath shaker a mass *m* (g) of the sorbent in polyethylene flasks containing a volume *V* (mL) of solution with different concentrations of uranium (50, 100, and 150 mg/L). The shaking speed is maintained at 200 rpm throughout the study. At the end, the sorbent is centrifuged for 5 min at 3500 rpm. The residual concentration of the ions left in the supernatant phase is determined using a UV-spectrometer following the Arsenazo III procedure [5,20]. The solution pH is adjusted to the required value ranging from 2 to 11 using a solution of 0.1 M HCl (37%) or 0.1 M NaOH (98%).

The sorption uptake and the equilibrium metal uptake capacity q_e (mg/g) are, respectively, calculated from the following expressions:

$$\text{Sorption uptake} = \frac{C_i - C_{eq}}{C_i} \times 100 \tag{1}$$

$$q_e = V \frac{C_i - C_{eq}}{m} \tag{2}$$

where C_i and C_{eq} are the initial and equilibrium concentrations of uranium ion (mg/L). *V* is the volume of the solution (L) and *m* is the mass of sorbent (g).

To optimize uranyl ion removal conditions, experiments are first performed using the synthetic solution. The obtained optimized parameters ($pH_{AEL} = 7$, $pH_{AFI} = 6$, contact time = 120 min and solid-to-liquid ratio of 0.1/150 (g/mL)) are then used as experimental conditions in the uranium sorption tests using nuclear effluents.

3. Results and discussion

3.1. Characterization of AEL and AFI adsorbents

The X-ray diffraction (XRD) patterns of the prepared AEL and AFI sieves are shown in Fig. 1. The obtained diffractograms indicate that the hydrothermally synthesized $AlPO_4$-5 and SAPO-5 are pure phase AFI and $AlPO_4$-11 and SAPO-11 are pure phase AEL with high crystallinity. The X-ray diffractograms are identical to those presented in the literature characterizing AFI and AEL crystalline phases [21,22].

The chemical composition obtained by the X-ray fluorescence analysis and the calculated charge of AFI and AEL sorbents are given in Table 1.

The surface area calculated according to the BET model and the pore volumes for the samples prepared are summarized in Table 1. One can notice that the AFI porous volume and surface area values are larger than the corresponding values for AEL sorbents.
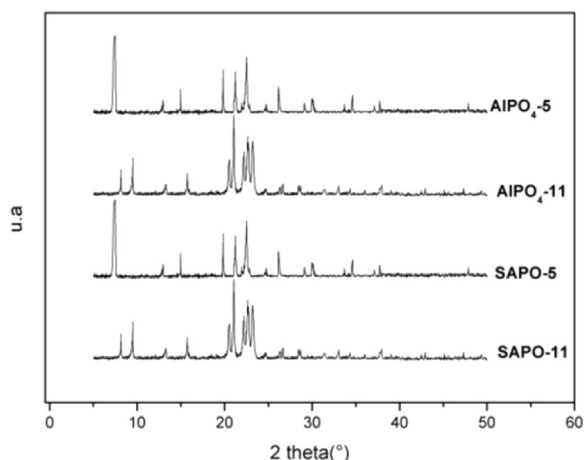
Fig. 1. X-ray diffraction patterns of calcined AlPO$_4$-5, SAPO-5, AlPO$_4$-11 and SAPO-11 sorbents.

Table 1
Textural characteristics and chemical compositions of AEL and AFI adsorbents.

Sorbents	S_{BET} (m^2/g)	V (cm^3/g)	Chemical composition	Charge/ TO$_2$
SAPO-5	230 ± 1	0.371 ± 0.001	Si$_{0.075}$ Al$_{0.489}$ P$_{0.436}$ O$_2$	−0.055
AlPO$_4$-5	220 ± 1	0.262 ± 0.001	Al$_{0.502}$ P$_{0.498}$ O$_2$	0
SAPO-11	153 ± 1	0.238 ± 0.001	Si$_{0.063}$ Al$_{0.489}$ P$_{0.448}$ O$_2$	−0.041
AlPO$_4$-11	148 ± 1	0.212 ± 0.001	Al$_{0.499}$ P$_{0.501}$ O$_2$	0

3.2. Application of AEL and AFI sorbents in nuclear effluents

The uranium sorption tests of the synthesized sorbents are performed using nuclear radioactive effluents collected from the Nuclear Research Centre of Draria (Algeria). The effluents are taken at different unit operations along the process of uranium purification and concentration in the uranium ore treatment. Three samples are collected and placed separately in polyethylene bottles of 450 cm^3 volume each. The bottles are completely sealed for more than 30 days to allow radioactive equilibrium to be reached. The measurement of uranium-235 activity is carried out using a detector hyper-pure germanium of 30% efficiency. The detector has a resolution of 1.9 keV at the ^{60}Co gamma-ray energy of 1332 keV. The gamma-ray spectrometer energy and efficiency calibration is performed using a ^{152}Eu source in a Marinelli beaker (multi-gamma volume source in a water-equivalent resin matrix). The samples are packaged in Marinelli-type containers, and the acquisition of gamma spectra duration is 86,400 s. The spectrum deconvolution software used is gamma vision of ORTEC, an example of gamma spectrum is given in Fig. 2. The elements and radioelement compositions of the three studied effluents are given in Table 2.

To test the effluent composition influence on uranium sorption, experiments were performed using real effluents and synthetic uranium solutions at 50, 100 and 150 mg/L under experimental conditions of pH$_{AEL}$ = 7, pH$_{AFI}$ = 6, contact time = 120 min and solid-to-liquid ratio of 0.1/150
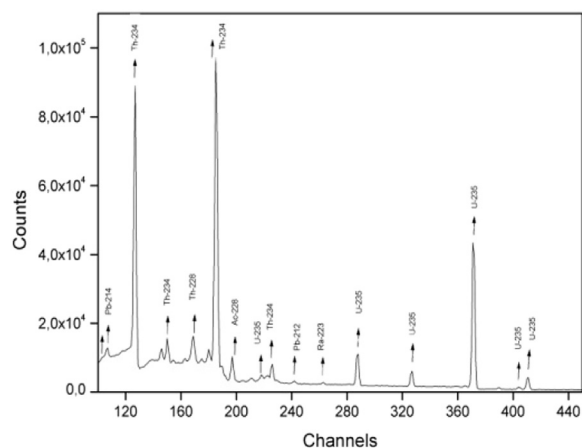

Fig. 2. Portion of the gamma-ray spectrum of effluent 2.

(g/L). The percentages of uranium (VI) ions' sorption from nuclear effluents and synthetic solutions onto SAPO-5, AlPO$_4$-5, SAPO-11 and AlPO$_4$-11 sorbents are presented in Fig. 3.

According to the obtained results presented in Fig. 3, the sorption rate of uranium (VI) follows the order: % SAPO-5 > % AlPO$_4$-5 > % SAPO-11 > % AlPO$_4$-11. The same trend is observed for both real effluents and synthetic solutions. It appears that AFI sorbents present the larger values of uranium uptake for all the solutions used in this study. This behaviour may be explained by the difference in the structure where SAPO-5 and AlPO$_4$-5 are part of a 12-membered ring pore structure, which permits uranium to diffuse out the pore at a relatively faster rate than onto SAPO-11 and AlPO$_4$-11, which belongs to a 10-membered ring pore structure [2]. Furthermore, the higher surface area and pore volume (Table 1) are responsible for the good sorption properties of the adsorbent with AFI structure. We can also notice, for the sorbents belonging to the same structure, the SAPO sorbent is more efficient than the AlPO; this behaviour may be explained by the silicoalumino-phosphate framework negative charge, which could favour the sorption of positively charged uranyl ion species in contrast to the neutral framework of aluminophosphate [3]. As can be seen from Fig. 3, uranium (VI) sorption uptake increases with initial uranium concentration for all sorbents used. This can be because of the increase in mass driving force from solution to the sorbent surface, which enhances the interaction between sorbate and sorbent [12,22]. For the same concentration used, the percentage of uranium (VI) ions is larger in the synthetic solution than in real effluent. This is mainly because of the presence of other *elements* in the effluents (Table 2), which can be cosorbed with uranium and compete with it to occupy the active sites for the sorbents [23]. Thus, the coexistence of various elements such as thorium, iron and manganese may compete for the sorption sites with uranium ions resulting in a substantial reduction of uranium removal. Indeed, it has been demonstrated that the inhibition of uranium sorption is because of the presence of thorium and iron, which are considered as the most potent competitors of uranium for sorptive sites [24,25].

Table 2
The elements and radioelement compositions of the effluents.

Effluents	Nuclide	Average activity (Bq/L)	Energy (keV)	Element	Concentration (mg/L)
1	U-235	79.0	185.72	U	150
	Pb-214	05.8	351.99	Fe	63
	Ac-228	05.6	338.40	Mg	9.52
	Th-234	905.1	112.81	Cu	–
	Pb-210	23.1	46.52	Zn	–
	Pb-212	02.9	238.63	Mn	0.7
2	U-235	49.1	185.72	U	100
	Pb-214	03.5	295.22	Fe	62.5
	Ac-228	03.2	462.73	Mg	1.12
	Th-234	231.1	112.81	Cu	Traces
	Ra-223	01.3	122.40	Zn	Traces
	Pb-212	09.5	115.18	Mn	–
3	U-235	26.5	185.72	U	50
	Pb-214	01.5	351.99	Fe	41.14
	Ac-228	01.3	968.90	Mg	28.60
	Th-234	346.2	92.80	Cu	3.11
	Pb-210	02.0	46.52	Zn	12.83
	Pb-212	24.1	115.18	Mn	–
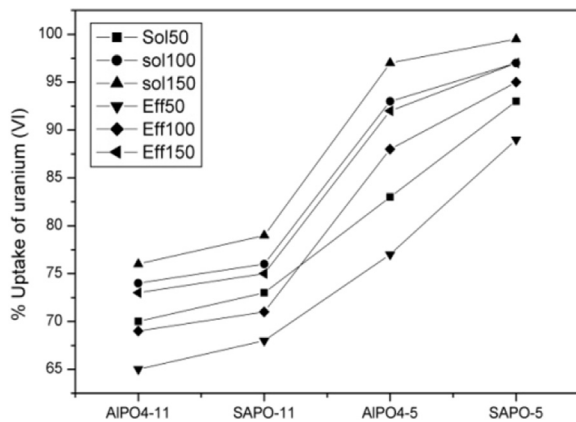
Fig. 3. The uranium uptake percentage from synthetic solution and real effluents sorbed onto AlPO$_4$-5, SAPO-5, AlPO$_4$-11 and SAPO-11.

3.3. Decontamination factor

Decontamination factor (DF) is a dimensionless quantity used to describe the ratio of the contamination level before treatment to that after treatment. It is very useful for the selection of suitable materials as sorbent and commonly used in waste management applications [26].

The DF is calculated using the following equation:

$$K_d = (DF - 1) \cdot \frac{V}{m} \qquad (3)$$

where K_d is the distribution coefficient, V the volume of liquid effluent and m is the amount of *sorbent*.

As can be seen from Table 3, DF values are more important for AFI sorbents, indicating a significant decontamination effect of both sorbents. This value increases with effluent activity and temperature. Moreover, SAPO-5 exhibits a higher DF value, showing that it is more suitable for uranium (VI) removal from nuclear effluents than AEL sorbents.

3.4. Thermodynamic study

The thermodynamic parameters, that is, enthalpy $\Delta H°$, entropy $\Delta S°$ and free energy $\Delta G°$ for the sorption of uranium (VI) ions onto AFI and AEL are calculated from the slope and the intercepts of $\ln K_d$ versus $1/T$ linear regression plots Fig. 4. The estimated values of the thermodynamic parameters for the sorption of uranium (VI) onto AFI and AEL sorbents are summarized in Table 4.

The observed positive values for the enthalpy $\Delta H°$ indicate the endothermic nature of the process. Moreover, the positive value for entropy $\Delta S°$ reflects the affinity of AFI and AEL sorbents to uranium (VI) removal. The negative $\Delta G°$ values observed for all sorbents show that the sorption process of uranium (VI) is spontaneous and the degree of spontaneity increases with increasing temperature.
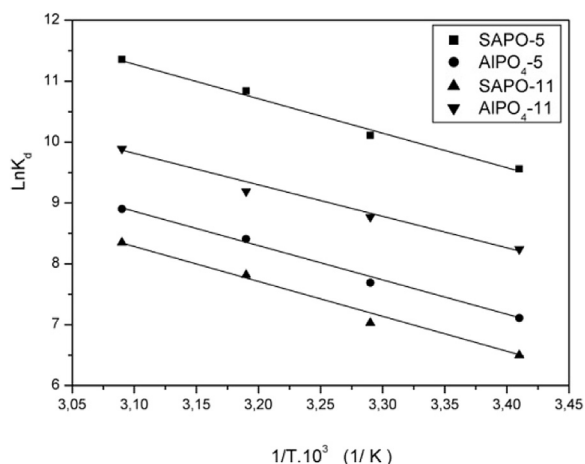
3.5. Sorption diffusion

In the objective to determine the sorption mechanism, the kinetic results obtained under experimental conditions (pH$_{AEL}$ = 7, pH$_{AFI}$ = 6, solid-to-liquid ratio of 0.1/150 g/L, [U] = 50 mg/L and time ranging from 5 to 240 min) are analysed by the intraparticle diffusion model expressed as

$$q_t = k_{id}t^{0.5} + C \qquad (4)$$

where q_t is the sorption capacity (mg/g) at time t and k_{id} is the intraparticle diffusion rate constant (mg g^{-1} min^{-1}). The values of the intercept C provide an indication on the thickness of the boundary layer. If the rate-controlling step is intraparticle diffusion, a plot of q_t versus $t^{0.5}$ should yield a straight line passing through the origin. The plot of q_t versus $t^{0.5}$ is shown in Fig. 5, where two straight lines with two different slopes are observed for SAPO-5, AlPO$_4$-5, SAPO-11 and AlPO$_4$-11. Clearly, the intraparticle diffusion is not applicable to the entire time scale of the sorption.

The first straight line corresponds to the external surface fast sorption. The second straight line is the gradual sorption stage. Similar two-stage kinetics was earlier reported [13]. The calculated intraparticle diffusion constants k_{id1}, k_{id2} and C_1 and C_2 are presented in Table 5.
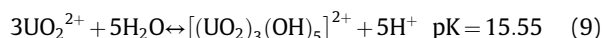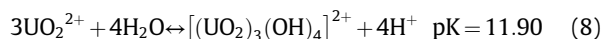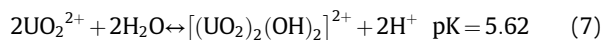
Table 3
Effluent decontamination factors of AEL and AFI sorbents.

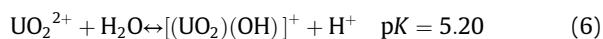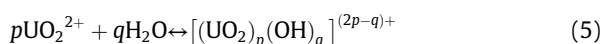| Effluents	U-235 activity (Bq/L)	Decontamination factor (DF)							
		SAPO-5		AlPO$_4$-5		SAPO-11		AlPO$_4$-11	
		293 K	323 K	293 K	323 K	293 K	323 K	293 K	323 K
1	26.5 ± 0.2	44.84	1000	5.36	100	3.60	17	3.33	14.28
2	47.1 ± 0.2	49.50	1667	11.86	200	3.89	25	3.54	20.00
3	79.0 ± 0.2	53.00	5000	24.78	500	4.70	50	3.75	33.33

Fig. 4. The thermodynamic parameters for the sorption of uranium (VI) onto AlPO$_4$-5, SAPO-5, AlPO$_4$-11 and SAPO-11 sorbents.

As expected, the diffusion rate k_{id1} in the first stage is larger than in the second (k_{id2}). Indeed, uranium (VI) is adsorbed quickly by the external surface via film diffusion. When the external surface reaches saturation, the uranium (VI) enters the internal pores [7].

The value of the intercept C provides information related to the thickness of the boundary layer. Larger values of the intercept obtained for SAPO-5 suggest that the surface diffusion has a larger role as the rate-limiting step [27]. This behaviour may be explained by both the AFI structure and uranium speciation.

The species of uranium are influenced by pH solution, different mononuclear and polynuclear U (VI) hydrolysis products in the form $[(UO_2)_p(OH)_q]^{(2p-q)+}$ as a function of pH values are present in uranium solution. The repartition is determined by the following equilibria:
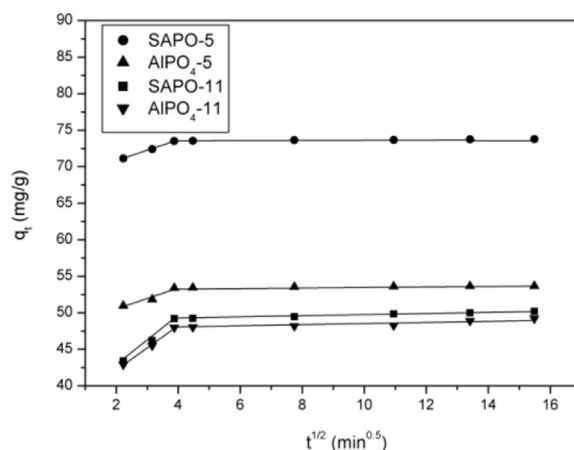
$$pUO_2^{2+} + qH_2O \leftrightarrow [(UO_2)_p(OH)_q]^{(2p-q)+} \tag{5}$$

$$UO_2^{2+} + H_2O \leftrightarrow [(UO_2)(OH)]^+ + H^+ \quad pK = 5.20 \tag{6}$$

$$2UO_2^{2+} + 2H_2O \leftrightarrow [(UO_2)_2(OH)_2]^{2+} + 2H^+ \quad pK = 5.62 \tag{7}$$

$$3UO_2^{2+} + 4H_2O \leftrightarrow [(UO_2)_3(OH)_4]^{2+} + 4H^+ \quad pK = 11.90 \tag{8}$$

$$3UO_2^{2+} + 5H_2O \leftrightarrow [(UO_2)_3(OH)_5]^{2+} + 5H^+ \quad pK = 15.55 \tag{9}$$

At pH between 3.0 and 5.0, the polynuclear products $[(UO_2)_2(OH)_2]^{2+}$, $[(UO_2)_3(OH)_4]^{2+}$ and $[(UO_2)_3(OH)_5]^+$ are

Fig. 5. Intraparticle diffusion plots for uranium (VI) sorption onto AlPO$_4$-5, SAPO-5, AlPO$_4$-11 and SAPO-11 sorbents.

Table 5
Intraparticle diffusion rate constants for uranium (VI) adsorption onto AEL and AFI sorbents.

Sorbents	k_{id1} (mg g^{-1} min$^{-0.5}$)	C_1 (mg/g)	k_{id2} (mg g^{-1} min$^{-0.5}$)	C_2 (mg/g)
SAPO-5	1.44	67.88	0.02	73.46
AlPO$_4$-5	1.46	47.56	0.02	53.37
SAPO-11	3.50	35.96	0.08	48.82
AlPO$_4$-11	3.07	35.43	0.03	47.91

present with UO_2^{2+} and $[UO_2(OH)]^+$ and are available for sorption. At pH higher than 6, the hydrolysis is more intense and other polynuclear product $[(UO_2)_4(OH)_7]^{+1}$ is formed [28]. All these species can be readily *sorbed* by the AFI and AEL sorbents. Moreover, at pH values higher than 7.0, carbonate uranyl ion $UO_2(CO_3)_2^{2-}$ and $UO_2(CO_3)_3^{4-}$ are formed [29,30]. The diameter of the hydrated uranyl is 6.5 Å, because the ionic radius of the uranyl ion is equal to 1.8 Å and the atomic radii of oxygen and hydrogen are 0.74 Å and 0.37 Å, respectively [5]. This diameter is less than that of the channels of the AFI and AEL structures, which consist of one-dimensional 12-membered ring pores (7.3 × 7.3 Å in size) and 10-membered ring pores (6.5 × 4.0 Å), respectively, that allow its diffusion in the AFI sorbents more favourably than onto AEL sorbents.

4. Conclusion

In the present study, AFI and AEL sorbents are synthesized successfully and characterized. According to the X-ray diffraction analysis the elaborated samples are pure phase

Table 4
Thermodynamic parameters for uranium (VI) sorption onto AEL and AFI sorbents.

Sorbents	$\Delta H°$ (kJ/mol)	$\Delta S°$ (J/mol K)	$\Delta G°$ (kJ/mol)			
			293 K	303 K	313 K	323 K
SAPO-5	47.88	242.51	−23.21	−25.63	−28.06	−30.48
AlPO$_4$-5	41.95	211.16	−19.95	−22.06	−24.17	−26.28
SAPO-11	47.63	221.40	−17.27	−19.48	−21.70	−23.91
AlPO$_4$-11	48.05	217.82	−15.80	−17.98	−20.16	−22.33

AFI and AEL with high crystallinity. The as-prepared materials are used in the sorption of uranium (VI) ion from nuclear effluents.

Attempts for effective removal of uranium (VI) from radioactive effluents with different activity obtained from Nuclear Research Center of Draria, Algeria using SAPO-5, AlPO$_4$-5, SAPO-11 and AlPO$_4$-11 sorbents are made. The uptake of uranium ions sorbed onto the sorbents varies between 70 and 98% for the investigated nuclear effluents activities. Furthermore, the DFs calculated are very important for high activity effluent. Moreover, SAPO-5 exhibits a higher DF value at 323 K. The thermodynamic studies show that the sorption process is spontaneous and endothermic because of the negative ΔG value and positive ΔH value. The analyses of the experimental kinetics data of the studied sorbents by the intraparticle diffusion model indicate that the uranium (VI) is sorbed quickly by the external surface via film diffusion, when the external surface reaches saturation; the uranium (VI) enters the internal pores. This study concludes that the elaborated SAPO-5, AlPO$_4$-5, SAPO-11 and AlPO$_4$-11 are suitable sorbent candidates for the removal of uranium. However, sorbent with AFI structure is a highly effective material for the removal of uranium (VI) ions from nuclear effluents.

Acknowledgements

References

[1] S.T. Wilson, B.M. Lok, E.M. Flanigen, US Patent, 4, 310, 440 (1982).

[2] E.M. Flanigen, Stud. Surf. Sci. Catal. 37 (1988) 13−27.
[3] J. Kornatowski, C. R. Chimie 8 (2005) 561−568.
[4] Ch. Baerlocher, W.M. Meier, D.H. Olson, Atlas of Zeolite Framewok Types, Elsevier Science, Amsterdam, 2001.
[5] A. Krestou, A. Xenidis, D. Panias, Miner. Eng. 16 (2003) 1363−1370.
[6] A.E. Osmanlioglu, J. Hazard. Mater. B 137 (2006) 332−335.
[7] M.K. Sureshkumar, D. Das, M.B. Mallia, P.C. Gupta, J. Hazard. Mater. 184 (2010) 65−72.
[8] F. Aydin, M. Soylak, Talanta 72 (2007) 187−192.
[9] N. Bayou, O. Arous, M. Amara, H. Kerdjoudj, C. R. Chimie 13 (2010) 1370−1376.
[10] D. James, G. Venkateswaran, T.P. Rao, Micropor. Mesopor. Mater. 119 (2009) 165−170.
[11] R. Donat, J. Chem. Thermodyn. 41 (2009) 829−835.
[12] P. Ilaiyaraja, A.K.S. Deb, K. Sivasubramanian, D. Ponraju, B. Venkatraman, J. Hazard. Mater. 250 (2013) 155−166.
[13] R. Akkaya, J. Environ. Radioact. 120 (2013) 58−63.
[14] A.T. Rodriguez, A.L. Velasco, J.A. Field, R.S. Alvarez, Water Res. 44 (2010) 2153−2162.
[15] A. Rahmati, A. Ghaemi, M. Samadfam, Ann. Nucl. Energy 39 (2012) 42−48.
[16] T.S. Anirudhan, S. Rijith, J. Environ. Radioact. 106 (2012) 8−19.
[17] F. Houhoune, D. Nibou, S. Amokrane, M. Barkat, Water Treat. 51 (2013) 5583−5591.
[18] S. Belkhiri, M. Guerza, S. Chouikh, Y. Boucheffa, Z. Mekhalif, J. Delhalle, C. Colella, Micropor. Mesopor. Mater. 161 (2012) 115−122.
[19] F.D. Snell, Photometric and Fluorometric Methods of Analysis: Metals, Wiley, New York, 1978.
[20] S.H. Jhung, Y.K. Hwang, J.S. Chang, S.E. Park, Micropor. Mesopor. Mater. 67 (2004) 151−157.
[21] H. Robson, K.P. Lillerud (Eds.), XRD Patterns, Verified Syntheses of Zeolitic Materials, Elsevier Science B.V., Amsterdam, 2001.
[22] K.M. Abd El-Rahman, M.R. El-Sourougy, N.M. Abdel Monem, I.M. Ismail, J. Nucl. Radiochem. Sci. 7 (2006) 21−27.
[23] D. Alipour, A.R. Keshtkar, M.A. Moosavian, Appl. Surf. Sci. 366 (2016) 19−29.
[24] S.M. Yakout, M.A. Rizk, Isot. Radiat. Res. 40 (2) (2008) 409−419.
[25] S. Abbasizadeh, A.R. Keshtkar, M.A. Mousavian, Chem. Eng. J. 220 (2013) 161−171.
[26] M.I. Ojov, W.E. Lee, An Introduction to Nuclear Waste Immobilization, Elsevier Science B.V., Amsterdam, 2005.
[27] H.K. Boparai, M. Joseph, D.M. O'Carroll, J. Hazard. Mater. 186 (2011) 458−465.
[28] S. Menacer, A. Lounis, B. Guedioura, N. Bayou, Desalin. Water Treat. 57 (34) (2016) 16184−16195.
[29] G.R. Choppin, J. Chem. 99 (2006) 83−92.
[30] J. Yu, J. Wang, Y. Jiang, Nucl. Eng. Technol. (2016) (in press).